UNIVERSITA' DEGLI STUDI DI BOLOGNA

Dipartimento di INGEGNERIA ELETTRICA

Gabriele Grandi

INFLUENCE OF SWITCH CHARACTERISTICS ON CONDUCTED DIFFERENTIAL-MODE INTERFERENCES IN POWER ELECTRONIC CONVERTERS

Research activities of Dr. Gabriele GRANDI (Univ. of Bologna) within the "*Leonardo*" Staff Exchange Program with EFI/NTNU - Trondheim (N)
• *July 4th - September 12th, 1996* •

DIE Internal Report ***October 1996***

INTRODUCTION

In recent years, the electromagnetic interference (EMI) problems have become a very important aspect in the design of electronic power converters. The complexity of even the simplest of circuits, necessitates the use of numerical tools for analyze and prediction of EMI. Several circuit oriented simulation programs are available and suitable in the study of conducted interferences. The main problem is to determine an equivalent circuit to represent accurately the converter behavior in a wide frequency range. At high frequencies (conducted interferences are considered up to 30 MHz) the presence of parasitic components cannot be neglected in the equivalent circuit modeling. This paper analyze the influence of power switch models on the differential-mode EMI spectrum. For this purpose, a proper equivalent circuit is considered to represent a simple switching cell (DC chopper). Line Impedance Stabilization Networks (LISNs) are employed to get the EMI signal according to the International Standard.

Aims of the work

- **General analysis of conducted EMI on the input-side of power converters.**
  In particular, a DC/DC buck chopper was considered as a basic switching cell (1 mosfet + 1 diode). Line Impedance Stabilization Networks (LISNs) are considered to standardize measurements.
  A detailed analysis of the HF current components flowing in the converter is presented.
- **Comparison of numerical results obtained by means of KREAN and PSPICE.**
  The comparison starts considering ideal switches. The effects of the switches model (mosfet and diode) are emphasized. The models of the switches in KREAN and PSPICE are compared. The comparison is also extended to a International Rectifier (IR) model of a MOSFET.
- **Proposal of simple switches models for PSPICE and KREAN simulations.**
  In particular, the finite turn-on and turn-off times, the off-state capacitances and the reverse recovery for the diode are taken into account. General considerations on the possibility to predict conducted EMI by means of numerical simulations are done.

INDEX

1. HF equivalent lumped parameter circuit for a switching cell

The equivalent circuit for a switching cell, one suitable to be employed in circuit-oriented simulation tools, is depicted in Fig. 1.1. The switching cell operates in forward conduction mode: the upper MOSFET performs the switching function while the lower MOSFET is kept off. Only the reverse parasitic diode of the lower MOSFET is active, and the lower MOSFET can then be replaced by a simple fast diode.

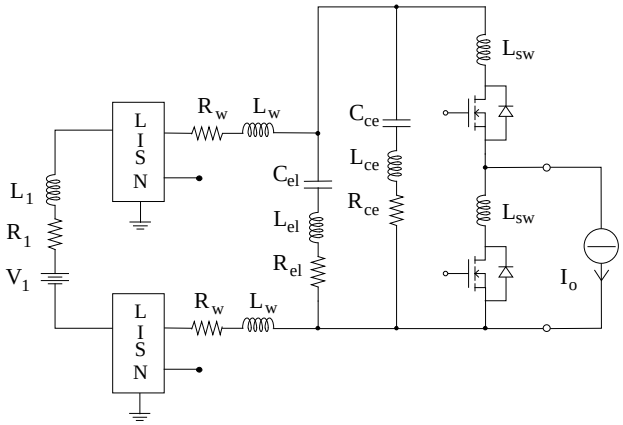

Fig. 1.1 - *Chopper equivalent circuit*

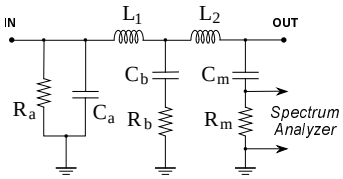

Fig. 1.2 - *LISN circuit*

Usually, on the source DC-side of the power converter, two kind of capacitors are connected as depicted in Fig. 1.1. The electrolytic capacitor (C_{el}) has a large capacitance value (i.e. thousands of μH) but also a large parasitic inductance (L_{el}). The ceramic capacitor (C_{ce}) has a lower capacitance (i.e. fractions of μH) but also a lower parasitic inductance (L_{ce}). The meaning of all the parameters in this circuit is also well explained in [1] and [2]. In this case, there is no connection between the heatsink of the power switches and the ground (there is no capacitive coupling to ground).

Between the DC source and the chopper, two Line Impedance Stabilization Networks (LISNs) are considered to reproduce the experimental set-up recommended to standardize measurements (Fig. 1.2). In fact, by specifying the serial impedance of the LISN to an appropriately high value, the impedance seen from the chopper (EMI source) will be largely independent of variations in the DC source impedance. The LISN establishes a standard profile of load impedance (resistive, 50 Ω at HF) toward the chopper and also filters out HF disturbances on the DC source that could create measurement problems [1], [3], [4].
Usually the LISNs are realized with components with extremely low parasitic effects and in this work the LISN's parasitic will be neglected.

The equivalent circuit shown in Fig. 1.1 does not represent the internal circuit models of the switches (MOSFET and diode). These models should take into account the finite turn-on and turn-off times, the off-state capacitances and the reverse recovery for the diode. All these aspects will be widely discussed farther on.

2. HF current components and resonance loops

The source of the conducted HF interferences is obviously the switching action performed by the upper MOSFET. The qualitative time-behavior of the switch current is represented in Fig. 2.1.

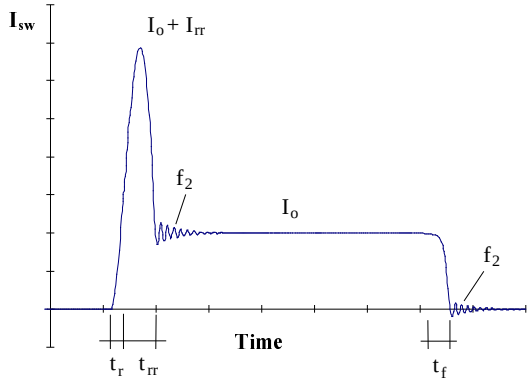

Fig. 2.1 - *Switch current (upper MOSFET)*

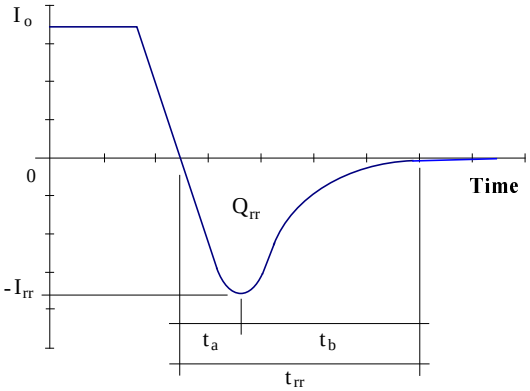

Fig. 2.2 - *Reverse diode current*

The main aspects that should be highlighted are:

- The rise time t_r and the fall time t_f.

  These times depend on the commutation speed of the MOSFET imposed by the gate signal and by the parasitic inductances in the commutating loop.

- The current peak.

  This peak is due to the reverse recovery in the diode (ref. to Fig. 2.2). Its amplitude ($I_{rr}+I_o$) and period ($t_{rr}=t_a+t_b$, a more datailed analysis can be found in [5]) depend on the commutating speed, parasitic inductances and turn-off characteristic of the free-wheeling diode (i.e. charge stored, Q_{rr}).

- The HF oscillations during turn-on and turn-off.

  This HF currents flows in the loop consisting of the power switches and the ceramic capacitor. Its frequency, f_2, is determined by the overall stray inductance of this loop and by the off-state capacitance of the MOSFET during the turn-off and by the off-state capacitance of the diode during the turn-on (after the reverse recovery), $f_2 = 1/2\pi\sqrt{LC}$. The damping factor is determined by the dissipative effects in the loop.

Unfortunately, the presence of both the ceramic and the electrolytic capacitors determine a LC loop and the switching action of the MOSFET starts a HF current oscillation in this loop. The frequency of this oscillation, f_1, is determined by the parasitic inductances in the loop and by the capacitance of the ceramic capacitor [2], [6].

3. Modeling the reverse recovery of the diode

In KREAN it is possible to model the first phase of the reverse recovery of a diode [7]. In particular, the reverse peak current I_{rr} can be specified. Unfortunately, once the current reaches $-I_{rr}$ the diode is turned off and the diode's resistance changes instantaneously from R_{on} to R_{off}. This abrupt change it's quite unrealistic and could also generate mathematical instabilities. For this reasons, it is not possible to introduce the diode reverse recovery in presence of a series inductance. In fact, it causes VHF oscillations of the diode current and high overvoltages due the abrupt change of the diode current in the second phase of the reverse recovery (such as an ideal switches). This problem can be overcame by introducing a RC snubber in parallel with the diode. Unfortunately, the capacitor can interfere with the other reactive components of the simulated circuit generating unrealistic HF behaviors. However, the value of the capacitance can be chosen according with the parasitic junction capacitance of the diode. To avoid the HF commutations of the diode, the value of the snubber resistance must be great enough (i.e., more than Ohms) to prevent the voltage inversion across the diode during the oscillations (a voltage inversion turns-on the diode and starts HF commutations). On the other hand, the value of the resistance must not be so high (i.e., no more than kilo-Ohms) to vanish the effects of the capacitor. A value ranging between tens and hundreds of Ohms can be selected in order to match also the desired di/dt in the second half of the reverse recovery (from $-I_{rr}$ to 0, time t_b). Higher values of this resistance determine low t_b with high di/dt and vice-versa. The first phase of the reverse recovery (the di/dt and the time t_a) is not affected by the values of the diode's RC snubber but it depends on the turn-on time of the upper switch and on the values of parasitic components in the commutating loop (i.e., inductances).
Also in PSPICE the models of discrete diodes do not handle the second phase of the reverse recovery. However, in the MOSFET models of PSPICE, the body-diode turns-off in a soft manner due to the high capacitive effects between drain and source. In this case the second part of the reverse recovery is realistic enough.
In order to avoid the sudden turn-off of the diode without additional capacitances, it is possible to consider external sub-circuits that can handle the second phase of the reverse recovery in a soft manner. Two different solutions can be considered:

1) Use an ideal diode adding the overall reverse recovery (both first and second phase)

2) Use the KREAN's or PSPICE's model adding only the second phase (soft recovery)

Solution 1

This solution can be applied at the ideal diode both in KREAN and in PSPICE. The corresponding circuit is represented in Fig. 3.1. It consists of an additional RC circuit driven by a current-controlled current source (gain K_1=1). A second current-controlled current source (gain K_2) adds the capacitor current to the diode branch providing for the reverse recovery. By adjusting the values of K_2 and C_c it is possible to modify the reverse current peak (I_{rr}) and the period of the second phase of the reverse recovery (t_b) while R_c=1.

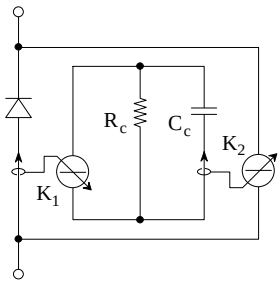

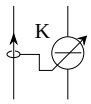

Fig. 3.1 - *Sub-circuit for the overall reverse recovery* *Current-controlled current source*

It could be observed that also in this case it is not possible to act on the first phase of the reverse recovery, as explained above (t_a and di/dt). A detailed relationship between the values of these parameter and the reverse current peak I_{rr}, the stored charge Q_{rr}, and the recovery time t_b can be found in [8].
This solution consents the sub-circuit to be completely decoupled from the diode branch and the unrealistic behaviors due to the additional capacitor are avoided.

Solution 2

Also this solution can be applied at the diode model in both KREAN and in PSPICE. The corresponding circuit is represented in Fig. 3.2. In this case the diode model handle the first phase of the reverse recovery while the external sub-circuit provides only for the second phase (soft recovery). It consists of an additional RL circuit driven by a current-controlled current source (gain K_1=1). A second current-controlled current source (gain K_2=1) adds the second phase of reverse recovery in a soft manner.

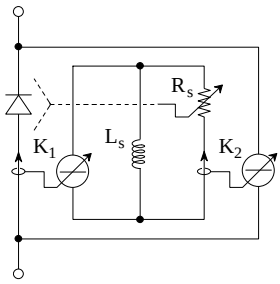

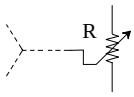

Fig. 3.2 - *Sub-circuit only for "soft recovery"* *Voltage-controlled binary switch*

The variable resistor is represented by the binary switch built-in in the libraries of both KREAN and PSPICE. The control variable is the on- or off-status of the diode that can be deduced by its voltage drop. The R_{on} value could be chosen at 2.2 Ω so that the value of the inductance L_s in nH equals the second period of the reverse recovery t_b in ns.
The R_{off} value is resulting from a compromise between accuracy (higher is better) and numerical convergence. It can be fixed at 500 Ω or more [9].
Also with this solution the sub-circuit is completely decoupled from the diode branch and the unrealistic behaviors due to the additional reactive components are avoided.

Utilizing one of the previous sub-circuits it is then possible to split the model of the diode in two parts: a model for the soft reverse recovery and a model for the capacitive effects. These models are decoupled one from the other. The simplest manner to take into account the capacitive effects consists of a RC branch in parallel with the diode. Now the values of both resistance and capacitance can be adjusted to match only the capacitive behavior of the diode. Other detailed model could also be employed to consider the variations of the capacitance with the reverse voltage across the diode [8].
It could be observed that to obtain realistic simulation results, the reverse recovery, in terms of both I_{rr} and t_a , has to depend on the switching speed of the upper MOSFET. In fact, the same reverse storage charge (Q_{rr}, the reverse current area) can be obtained in different ways by changing the di/dt. Using KREAN it appears then more proper to employ the first sub-circuit instead of the second in which I_{rr} is locked.

4. Modeling the commutations of the MOSFET

In KREAN's basic switch module the switching time is not modeled, so the commutation between R_{on} and R_{off} is instantaneous. To takes care of both the finite switching time and the upper MOSFET output capacitance, a RC snubber could be considered.
During the turn-off of the switch, the value of the snubber resistance determines the amplitude of the HF oscillations (the amplitude of the second resonant peak at frequency f_2). By increasing the value of this resistance, a greater smoothing factor is obtained and the commutation is faster. To obtain a smoothing effect also during the turn-on of the switch (this strongly affects the diode reverse recovery), the value of the snubber resistance should be much lower than the on-state resistance of the switch (R_{on}). Only in this way the snubber capacitor smoothes the voltage transient across the switch between V_{on} and V_{off} . Considering that the on state resistance is in the order of magnitude of hundreds of mΩ and the switching time are in the range of 10-1000 ns, the value of the snubber capacitor needed to match the time constant RC should be 0.1-10 μF. Unfortunately, the off-state capacitance of the power switches (such as MOSFETs or IGBTs) is in the order of 1 nF and then about three order of magnitude smaller. For these reasons, to model the turn-on time with a parallel RC snubber it's really a hard task.
In KREAN it is also possible to employ a switch module with a limit in the rate of change of the current (di/dt) during turn-on and turn-off. A trapezoidal shape instead of a rectangular shape for the current is then obtained. It could be observed that, in this case, the current behavior during the commutations depends only on the prefixed di/dt and it is not affected by the external circuit around the switch. In most cases it could be quite unrealistic.

The PSPICE's built-in model of an ideal switch allow to continuously change the switch resistance between R_{on} and R_{off} during a prefixed time selectable by the user. The current behavior during turn-on and turn-off is then determined by both the resistance transient and the external circuit characteristics. Using the PSPICE's model it is then possible to simulate the rise and fall times of the MOSFET in a satisfactory manner.
Also in this case, RC snubbers can be usefully considered to model the MOSFET output capacitance. The frequency (f_2) and the amplitude of the second resonant peak in the conducted EMI spectrum can be matched by selecting a proper value for the capacitance and for the resistance, respectively.

5. Numerical Results

In order to carry out numerical simulations with KREAN and PSPICE, a realistic set of the parameters shown in Fig. 1.1 has been chosen as follow

V_1=100 V	C_{el}=3300 μF	C_{ce}=0.33 μF	L_{sw}=10 nH	I_o=10 A
L_1=0.1 μH	L_{el}=100 nH	L_{ce}=10 nH	R_{sw}=0.1 Ω	
R_1=0.1 Ω	R_{el}=0.1 Ω	R_{ce}= 0.1 Ω		

According with the International Standards, the conducted EMI signal is taken from the LISN measuring terminals with a load resistance of 50 Ω representing the input impedance of the spectrum analyzer [1], [3], [4]. In all the following simulations, the switching frequency is 40 KHz with a duty cycle of 60%. These parameters do not affect the conducted EMI spectrum and therefore will be unchanged. The diagrams represent the EMI signal in a logarithmic scale (100 μV÷1 V that correspond to 40 dBμV÷120 dBμV) as function of the frequency (linear scale, up to 40 MHz).

5a. Conducted EMI with ideal switches

In this first case, the circuit has been considered with ideal switches. In both KREAN and PSPICE simulation tools, it's possible to consider controlled switches as binary resistors. The on- and the off-states are represented by different values of a series resistance (R_{on} and R_{off}). The commutation between R_{on} and R_{off} is instantaneous in the KREAN's model while it can be selected with a smooth variation between the ending values in the PSPICE's model. Now instantaneous commutations are considered. The input wires inductance L_w is neglected and will be examined later.

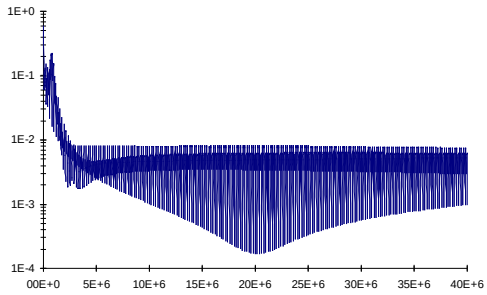

Fig. 5a.1a - *KREAN: Ideal Switches*

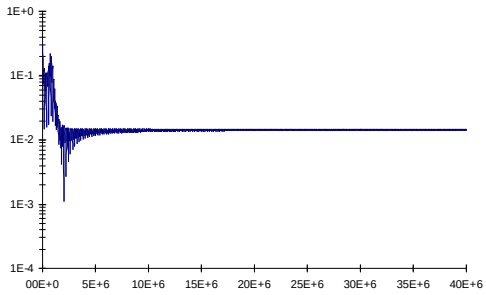

Fig. 5a.1b - *PSPICE: Ideal Switches*

In Figs. 5a.1a and 5a.1b are represented the conducted EMI spectra obtained with KREAN and PSPICE, respectively.
As stated above, the peak at about 800 KHz (f_1) is due to a resonance in the loop consisting of the electrolytic and the ceramic capacitors. This frequency can be calculated with the simple LC resonant-frequency formula.
The white noise is related to the overvoltages (spikes, very close to Dirac pulses) during the switches commutations (all the inductances have a parallel resistance of 100 KΩ).
The agreement between KREAN and PSPICE simulations is good. The computational times are very similar. It could be observed that in this case the simulators have well handled the overvoltages without convergence troubles.

In this simple case it is possible to highlight the effects of the wires parasitic inductance L_w between the LISNs and the chopper. In Figs. 5a.2a and 5a.2b are shown the results obtained by means of PSPICE considering inductances of 1 μH and 5 μH, respectively. Similar results was obtained with KREAN and are not represented here.

PSPICE: Ideal switches and input wires inductance

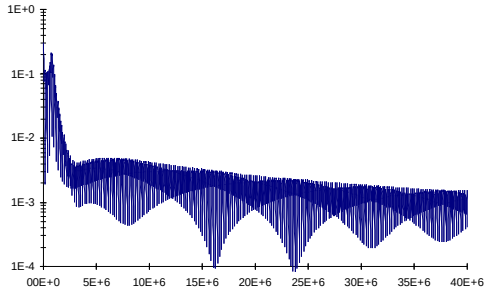

Fig. 5a.2a - *L_w=1μH*

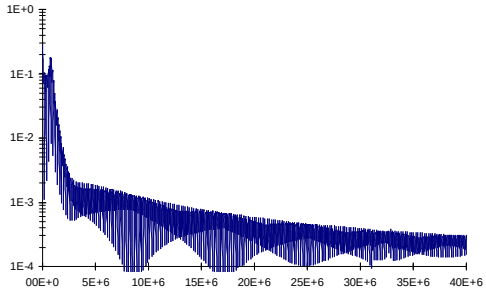

Fig. 5a.2b - *L_w=5μH*

As it is possible to see from these figures, the series wires inductance between chopper and LISNs does not introduce further resonances and, as expected, smoothes the HF interferences. In the following the presence of the input wires inductances will be neglected in order to highlight the HF harmonic content.

5b. Effects of the commutation time

The influence of the switching time in the case of binary switches can be deduced from the following figures.

PSPICE: Binary switches with different switching times

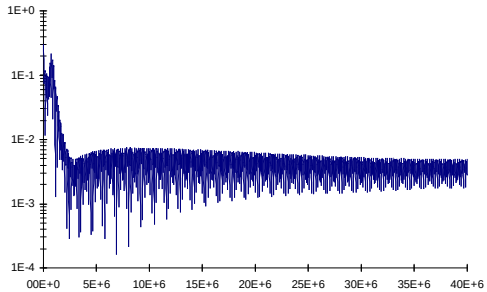

Fig. 5b.1a - *Switching times: $t_r = t_f = 0.2$ us*

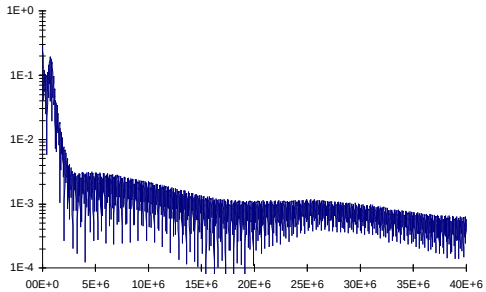

Fig. 5b.1b - *Switching times: $t_r = t_f = 1$ us*

In Figs. 5b.1 are shown the conducted EMI spectra obtained by means of PSPICE with a smooth variation of the switch resistance between R_{on}=0.1 Ω and R_{off}=100 KΩ. The switching times are 0.2 μs and 1 μs respectively.
Comparing these figures with the previous Fig. 5a.1a (ideal commutations) it is possible to see that an increasing in the switching times leads to a lower HF interferences level. In particular, the first resonant peak only slightly decreases but a higher decrease it observed for the VHF harmonic components. In fact, with a switching time grater then zero, the amplitude of the voltage spike across the switching inductances L_{sw} decreases and the white noise is smoothed.

The basic switch model of KREAN does not allow to change continuously the switch resistance during the commutations. The commutation model of the switch module in KREAN is quite different. As stated in section 4, it is possible to limit the di/dt during the turn-on and the turn-off. In the following figures 5b.2 and 5b.3 are compared the results obtained with both KREAN and PSPICE with the same average slope of the currant during the commutations.

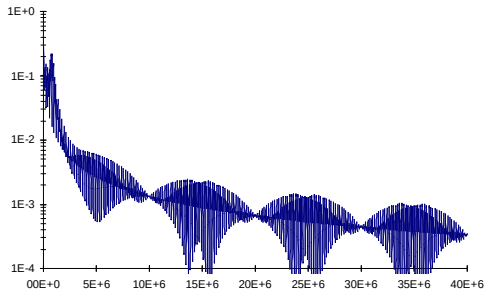

Fig. 5b.2a - *KREAN: di/dt=100 A/μs*

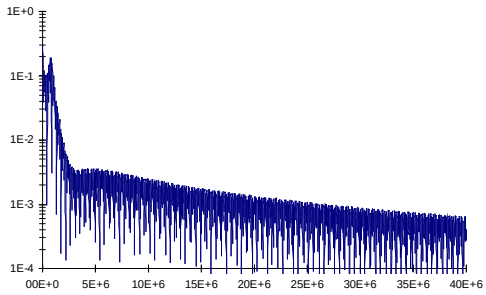

Fig. 5b.2b - *PSPICE: avg. di/dt=100 A/μs*

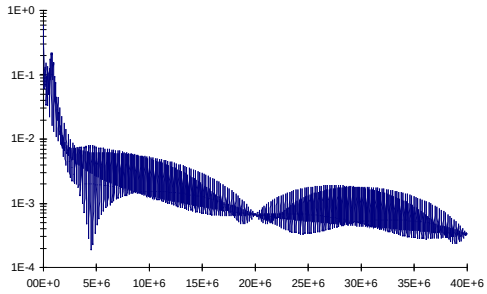

Fig. 5b.3a - *KREAN: di/dt=200 A/μs*

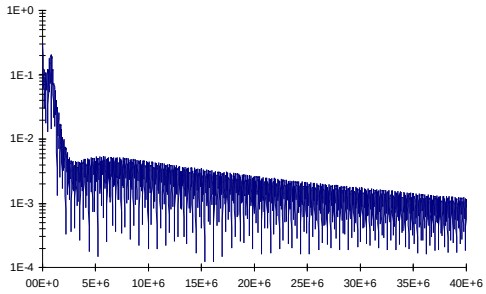

Fig. 5b.3b - *PSPICE: avg. di/dt=200 A/μs*

As it is possible to see from these figures, only the average behavior of the EMI spectrum is almost the same. With the switch module of KREAN are evident the periodical curvatures due to the trapezoidal shape of the switch current. In fact, the period in the frequency domain of these curves equal the theoretical values simply obtained by inverting the switching time: $f_c = 1/\tau$ (a more detailed analysis can be found in [4]).

In the first case, Fig. 5b2a, the switching time is
$\tau = I_o/(di/dt) = 10A/(100A/\mu s) = 100$ ns ----> $f_c = 10$ MHz.

In the second case, Fig. 5b.3a, is
$\tau = I_o/(di/dt) = 10A/(200A/\mu s) = 50$ ns ----> $f_c = 20$ MHz.

The amplitude of the first resonant peak (f_1=800 KHz) is still practically not affected by the commutation time.

5c. Conducted EMI with detailed switches models

In order to verify the effects of the switches model on the conducted EMI spectrum, a power MOSFET IRFP250 (rated at 200 V, 30 A) has been chosen from inside the built-in PSPICE models library. Also a different PSPICE model for the IRFP250, found in the International Rectifier (IR) library (http:\\www.irf.com), has been employed. The result obtained with a gate resistance R_g=33 Ω are represented in Figs. 5c.1a and 5c.1b.

PSPICE: simulations with different switches models

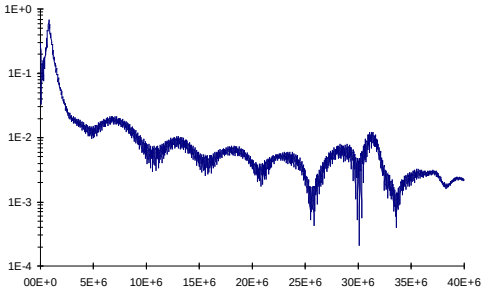

Fig. 5c.1a - *Built-in models of switches*
I_{rr}=56 A, t_a=92ns, t_b=190 ns

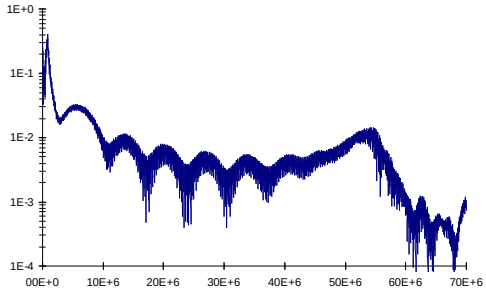

Fig. 5c.1b - *IR models of switches*
I_{rr}=56 A, t_a=74ns, t_b=63 ns

The built-in model and the IR model of this kind of MOSFETs have different behavior. In particular, although the reverse recovery current peak (I_{rr}) has the same amplitude, the reverse recovery time is much smaller in the former case ($t_{rr}=t_a+t_b$). This difference cause the different behavior between the lower (f_1) and the higher (f_2) resonant frequencies. It will be discussed later how the reverse recovery affects the EMI harmonic spectrum with more details. Also the output capacitance seems to be different. In fact, the higher resonant frequency is shifted from 32 MHz to 55 MHz (note the different frequency scale of the diagrams). In these terms, the built-in model seems to be more realistic, it matches better the value of the output capacitance given from the data sheet (C_{oss}=0.8 nF).
Comparing these diagrams with the ones obtained with ideal switches (Figs. 5a.1, it appears evident the influence of the switches model on the conducted EMI spectrum. The amplitude of the first resonant peak (at frequency f_1) is much greater and appears a second resonant peak (f_2). Also a particular behavior between these peaks can be observed. It consists in almost regular cavities and raises with amplitude decreasing when the frequency increases.

It should be noted that these models of MOSFET were not made for EMI simulation purposes but they are general-purpose models. In particular, the following effects are modeled (taken from PSPICE's Book):

- DC transfer curves in forward operation,
- gate drive characteristics and switching delay,
- "on" resistance,
- reverse-mode "body-diode" operation.

The factors not modeled include:

- maximum ratings (e.g. high-voltage breakdown),
- safe operating area (e.g. power dissipation),
- latch-up,
- noise.

We can observe that some of these effects are unnecessary for EMI prediction, in particular the gate drive input characteristic and the detailed on-state output behavior.
These models contain at least 20 different components in the sub-circuit (such as resistors, variable capacitors and controlled sources). To adjust the values of these parameter, in order to match better the model behavior with the experimental results, it's really a hard task.
All these considerations lead to understand that a specific switch model proper for EMI simulations could be a better solution. These model has to be simple enough to allow to match the main MOSFET characteristics by adjusting the values of few parameters. These characteristics consists mainly in

- on-state output resistance
- off-state output capacitive effects
- turn-on and turn-off times
- body-diode reverse recovery and forward voltage drop

5d. Effects of the diode model

In order to highlight the effects of the free-wheeling diode model on the conducted EMI spectrum, it's possible to consider the same structure of the chopper discussed above (section 5c) by substituting the lower MOSFET model with an ideal diode model.

PSPICE: simulations with mosfet model and IDEAL DIODE

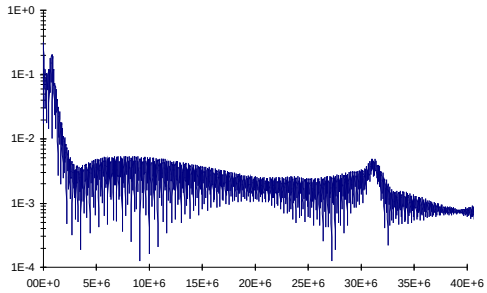

Fig. 5d.1a - *Built-in model of MOSFET*

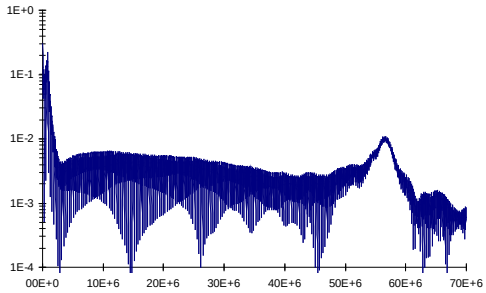

Fig. 5d.1b - *IR model of MOSFET*

The result of these simulations are represented in Figs. 5d.1. Comparing these figures with the corresponding 5c.1, it is possible to verify what has been previously stated: the diode model affects the first resonant peak amplitude and the behavior between the resonant peaks. The second resonant peak is slightly affected by the diode model.

In order to verify the effects of the reverse recovery, the sub-circuit represented in Fig. 3.1 (solution n. 1) is added to the ideal diode to provide for the reverse behavior. The PSPICE's built-in model is considered for the upper MOSFET.

PSPICE: mosfet model and DIODE with REVERSE RECOVERY

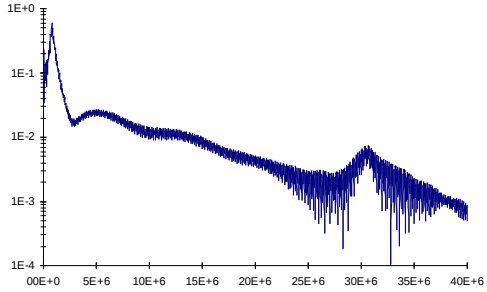

Fig. 5d.2a - *t_{rr}=260 ns and I_{rr}=59 A*

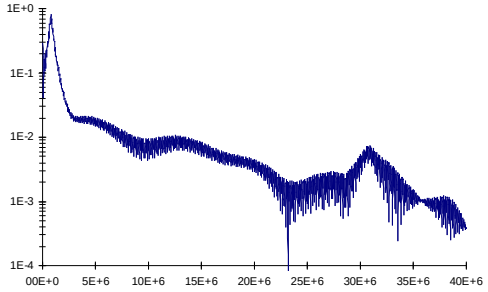

Fig. 5d.2b - *t_{rr}=420 ns and I_{rr}=59 A*

Figs. 5d.2 show the conducted EMI spectra considering about the same reverse current peak obtained with the body-diode model (I_{rr} = 56 A, ref. to Fig. 5c.1a).

In Fig. 5d.2a the parameters of the sub-circuit are fixed at K_2=12 and C_c=70 nF, the corresponding reverse recovery characteristics are t_a=90 ns, t_b=170 ns (t_{rr}=260 ns) and I_{rr}=59 A. In Fig. 5d.2b the parameters of the sub-circuit are fixed at K_2=10 and C_c=140 nF, the corresponding reverse recovery characteristics are t_a=100 ns, t_b=320 ns (t_{rr}=420 ns) and I_{rr}=59 A.

According with the considerations made in section 3.1, it could be observed that changing the sub-circuit parameters only the time t_b of the second phase of the reverse recovery can be usefully modified.
Comparing these figures with the previous Fig. 5d.1a it appears that the reverse recovery introduce an irregular behavior and shift-up the overall harmonics content. In particular, the amplitude of the first resonant peak increase when the reverse recovery increases. It's so possible to match the same results obtained with the body-diode model included in PSPICE (Fig. 5c.1a).

5e. Effects of the MOSFET model

In order to highlight the effects of the model of the MOSFET on the conducted EMI spectrum, it's possible to consider the same chopper structure as in section 5b only substituting the upper MOSFET model with an ideal switches. The following simulations, carried out by means of PSPICE, consider ideal switches (binary) with different transition times. The capacitive effects are taken into account with a parallel RC snubber.
The on-resistance of the binary switch, R_{on}, has been fixed to 0.1 Ω according to realistic values of these size of MOSFETs. The off-resistance, R_{off}, has been chosen at 100 KΩ, in this way the off-state leakage current does not affect the chopper behavior and numerical drawbacks are avoided.

PSPICE: simulations with IDEAL SWITCH and body-diode model

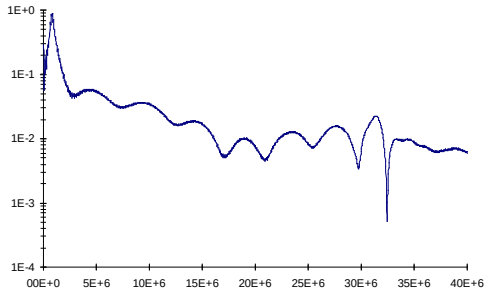

Fig. 5e.1 - *Ideal switch ($t_r = t_f = 1$ ns)*

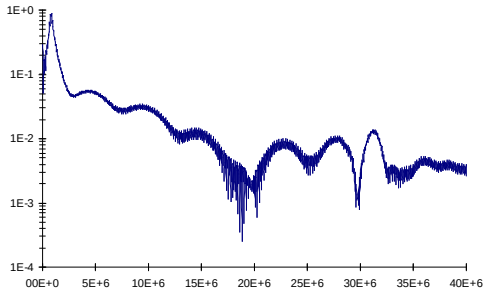

Fig. 5e.2 - *Switching times: $t_r = t_f = 0.1$ us*

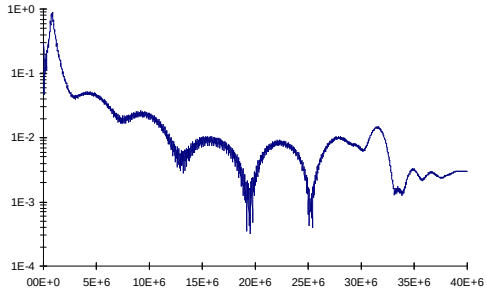

Fig. 5e.3 - *Switching times: $t_r = t_f = 0.2$ us*

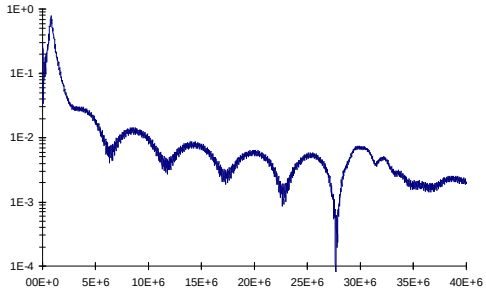

Fig. 5e.4 - *Switching times: $t_r = t_f = 0.5$ us*

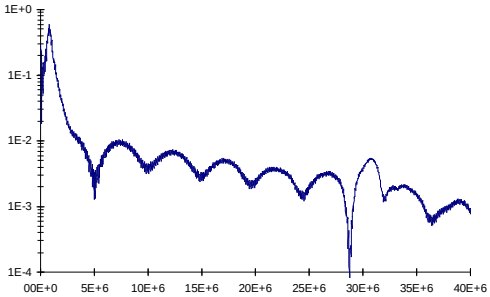

Fig. 5e.5 - *Switching times: $t_r = t_f = 1$ us*

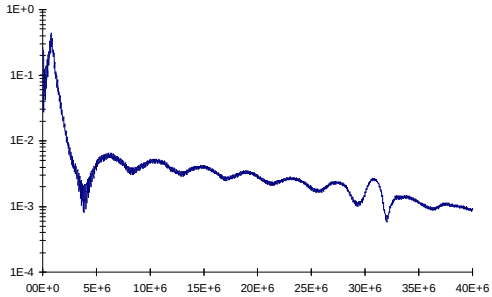

Fig. 5e.6 - *Switching times: $t_r = t_f = 2$ us*

In the figures from 5e.1 to 5e.6 are shown the conducted EMI spectra for different commutation times of the upper switch, starting with near-ideal commutation (1ns).

The switching time affects the reverse recovery time t_{rr} and reverse current peak I_{rr}. Reducing the switching time (faster commutations), t_{rr} decreases while I_{rr} increases from 28 A ($t_r = t_f = 2$ us) to 118 A ($t_r = t_f = 0.1$ us) (125 A with ideal switch, $t_r = t_f = 1$ ns).
As it is possible to see, the switching speed (and so the reverse recovery) also affects the amplitude of the first resonant peak (f_1=800 KHz): its amplitude increases for higher switching speed which corresponds to higher reverse peak current.
The shape of the EMI spectrum shows more evident curvatures (cavities and raises) for higher values of the switching speed. Their period, in the frequency domain, is higher for lower switching times and it appears that all the EMI spectrum is shifted-up.
The capacitive effects of the lower MOSFET (body-diode), responsible of the second resonant peak at f_2 = 32 MHz, are poor and they are just visible in the EMI spectra.

In order to understand the influence of the capacitive effects of the upper MOSFET, a RC snubber connected in parallel with the switch is now considered.
The value of the capacitance has been chosen according with the output MOSFET's capacitance from data-sheet ($C_{oss} = 0.8$ nF). The value of the resistance can be selected to introduce different damping factors.
The following figures 5e.7 and 5e.8 show the comparison between results both with and without RC snubber, *a* and *b* respectively.

PSPICE: effects of the IDEAL SWITCH RC snubber

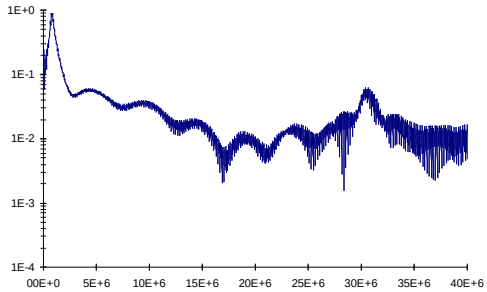

Fig. 5e.7a - *C=0.8 nF, R=20 mΩ, $t_r = t_f = 1$ ns*

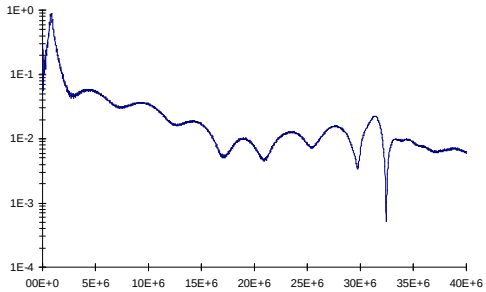

Fig. 5e.7b - *No RC, $t_r = t_f = 1$ ns*

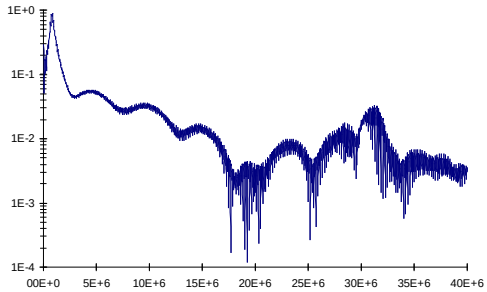

Fig. 5e.8a - *C=0.8 nF, R=20 mΩ, $t_r = t_f = 0.1$ μs*

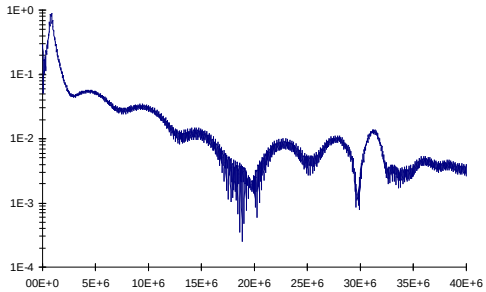

Fig. 5e.8b - *No RC, $t_r = t_f = 0.1$ μs*

From these figures it can be seen that the second resonance peak is due mainly to the parasitic capacitor of the upper MOSFET. The snubber resistance affects the amplitude of this peak (higher for lower resistances). The presence of the snubber does not change significally the reverse recovery.

5f. Simple models for MOSFET and diode

In this section are analyzed the results obtained by means of KREAN and PSPICE, where simple models for the MOSFET and the diode are implemented.
On the basis of the previous considerations, it appears that the three most important aspects that affects the conducted EMI are:

- Turn-on and turn-off switching times of the upper MOSFET
- Output capacitance of the upper MOSFET
- Reverse recovery of the diode

In Figs. 5f.1 are shown simulations obtained by means of KREAN and PSPICE neglecting the switching times (ideal commutations, τ=0). The model for the upper MOSFET consists of an ideal switch with R_{on}=0.1 Ω, R_{off}=100 KΩ and a parallel snubber with R=0.1 Ω, C=0.8 nF. The diode model consists of an ideal diode with the additional sub-circuit as represented in Fig. 3.1 to handle the reverse recovery. The values of the reverse recovery sub-circuit parameters are K_2=12 and C_c=70 nF.

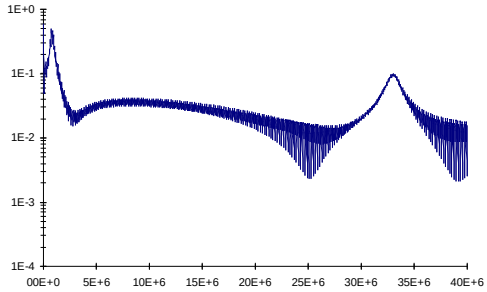

Fig. 5f.1a - *Simulation with KREAN, τ=0*

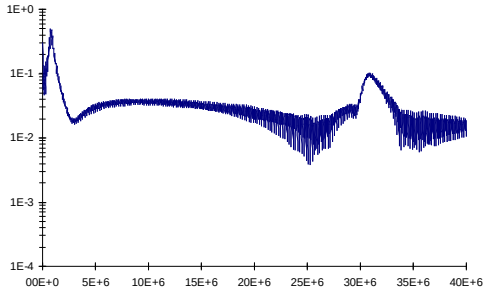

Fig. 5f.1b - *Simulation with PSPICE, τ=0*

From Figs. 5f.1a and 5f.1b results a good agreement between KREAN's and PSPICE's simulations. The irregularities in the second resonant peak (PSPICE) are probably due to its correspondence with a periodical cavity due to the reverse recovery. This correspondence can be seen better by examining the EMI spectrum in a wider frequency range as shown in Fig. 5f.2. Only the simulation result of PSPICE is reported since the Fourier analysis of KREAN is limited at 40 MHz (a maximum of 1000 harmonics, now the use of external numerical tools for the Fourier analysis is neglected).

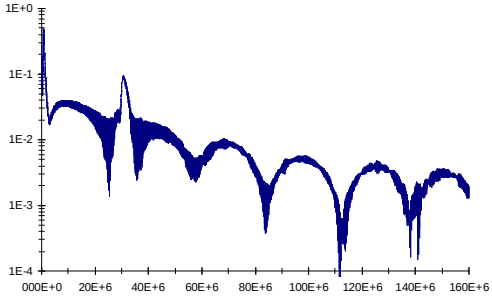

Fig. 5f.2 - *Simulation with PSPICE in a wide frequency range*

Introducing a commutation time grater than zero the following results are obtained. In particular, the switch module of KREAN is set with the current derivative limit at 100 A/μs (Fig. 5f.3a). Also the binary switch model of PSPICE with a smoothed transition between R_{on} and R_{off} is considered (Fig. 5f.3b).

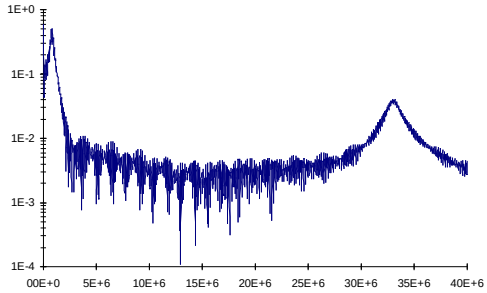

Fig. 5f.3a - *Simulation with KREAN*

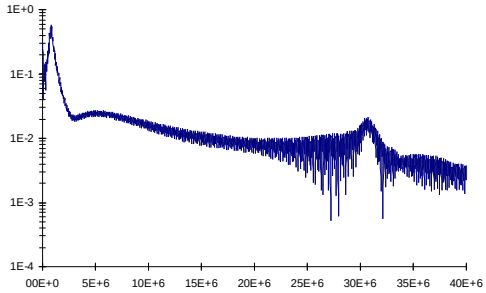

Fig. 5f.3b - *Simulation with PSPICE*

Comparing these figures with the previous 5f.1, it is possible to see that by increasing the switching times from zero to a finite value, a reduction of the HF interferences is obtained as already shown in section 5b. Now, also the effects of the switching times on both the second resonant peak (f_2) and reverse recovery can be emphasized.

In KREAN, the amplitude of the second resonant peak decreases. As expected, also the reverse recovery current peak decreases due to the reduced di/dt: from I_{rr}=95 A (with ideal switching, τ=0) to I_{rr}=30 A. Furthermore, in KREAN disappears the periodic curvatures in the spectrum (ref. to Fig. 5b.2a). This is an effect of the reverse recovery that modify the trapezoidal shape of the switch current.

In PSPICE the amplitude of the second resonant peak presents a greater decrease. The decrease in the reverse recovery current peak is lower: from I_{rr}=95 A (with ideal switching, τ=0) to I_{rr}=70 A. This characteristics of PSPICE can be explained by examining the current shape due to the variable resistance model of the binary switch in this circuit. The switch current presents a low di/dt at the beginning of the turn-on and at the end of the turn-off. This value of di/dt is strictly related to the selected switching times. The di/dt at the end of the turn-on and at the beginning of the turn-off is much higher and it is only slightly dependent on the selected switching time. The reverse recovery current, being affected by the di/dt in the last part of the turn-on, is very high and only slightly affected by the selected turn-on time. Indeed, the amplitude of the second resonant peak is affected by the di/dt in the last part of the turn-off (oscillations due to the RC snubber in parallel with the upper switch) and then is strongly dependent on the selected turn-off time.

6. Conclusions

In this work a detailed analysis of the conducted EMI generated by a switching cell has been done by means of numerical simulations. Both KREAN and PSPICE have been considered and the numerical results was compared. The main aspect that could be highlighted are the following:

- KREAN and PSPICE give very similar results in about the same computational times for predicting conducted EMI. Sometimes PSPICE has convergence trouble, the robustness of KREAN appears higher.
- Both KREAN and PSPICE have a switch model that take into account of the commutation times. These models are quite different and a combination of both seems to be the best solution to model the commutation of a real power MOSFET.
- The models of MOSFET available are general-purpose models and a very high number of parameters has to be fixed. It seems to be a better solution to build more simple models specific for conducted EMI simulations and predictions.
- To predict accurately the conducted interferences is a hard task. However, simulations can highlight very well the influence of both the parasitic parameters and the power switches characteristics on the conducted EMI spectrum. In this way, the designer of power converters can determine by simulations how to reduce or modify the HF behavior of the converter.

7. References

[1] L.Tihanyi: *Electromagnetic compatibility in power electronics*. IEEE Press 1995, New York (USA)

[2] G.Grandi, U.Reggiani, D.Casadei: *Modeling, simulation and experimental analysis of conducted EMI for a switching cell*. OPTIM, Brasov, May 15-17, 1996, Proc. pp 889-896

[3] P.A.Chatterton, M.A.Houlden: *EMC Electromagnetic theory to practical design*. WILEY 1992, Chichester, West Sussex (UK)

[4] C.R.Paul: *Introduction to Electromagnetic Compatibility*. WILEY 1992, New York

[5] N.Mohan, T.M.Undeland, W.P.Robbins: *Power Electronics: CONVERTERS, APPLICATIONS AND DESIGN*. WILEY 1989, Singapore

[6] F.Klotz, J.Petzoldt, H.Volker: *Experimental and simulative investigations of conducted EMI performance of IGBT for 5-10 KVA converters*. PESC, Baveno (IT) June 23-27, 1996, Proc. pp. 1986-1991

[7] O.Mo, R.Nilssen: *Low cost program for simulation of power electronic converters and systems*. EPE, 13-16 Sept. 1993, Brighton (UK), proc. pp. 29-34

[8] E.Labouré, F.Costa, C.Gautier, W.Melhem: *Accurate simulation of conducted interferences in isolated DC to DC converters regarding to EMI standards*. PESC, Baveno (IT) June 23-27, 1996, Proc. pp. 1973-1978

[9] F.Bertha, B.Velaerts, E.Tatakis: *An improved power diode model for PSspice, applied to converter simulation*. EPE, 13-16 Sept. 1993, Brighton (UK), Proc. pp. 249-254